

SUBSTRATE-MEDIATED FIDELITY MECHANISM ENSURES ACCURATE DECODING OF PROLINE CODONS

Byung Ran So^{1,4}, Songon An^{5,‡}, Sandeep Kumar^{1,4}, Mom Das^{1,3,4}, Daniel A. Turner¹, Christopher M. Hadad¹, and Karin Musier-Forsyth^{1,2,3,4}

Departments of ¹Chemistry and ²Biochemistry, ³The Ohio State Biochemistry Program, and ⁴Center for RNA Biology, The Ohio State University, Columbus, OH 43210; ⁵Department of Chemistry, University of Minnesota, Minneapolis, MN 55455

Correspondence should be addressed to: Karin Musier-Forsyth, Department of Chemistry, The Ohio State University, 100 West 18th Ave., Columbus, OH 43210, USA

Tel.: 614-292-2021; Fax: 614-688-5402; E-mail: musier@chemistry.ohio-state.edu

[‡]Current address: Department of Chemistry, The Pennsylvania State University, University Park, PA 16802, USA

Aminoacyl-tRNA synthetases attach specific amino acids to cognate tRNAs. Prolyl-tRNA synthetases (ProRSs) are known to mischarge tRNA^{Pro} with the smaller amino acid alanine, and with cysteine, which is the same size as proline. Quality control in proline codon translation is partly ensured by an editing domain (INS) present in most bacterial ProRSs that hydrolyzes smaller Ala-tRNA^{Pro} and excludes Pro-tRNA^{Pro}. In contrast, Cys-tRNA^{Pro} is cleared by a free-standing INS domain homolog, YbaK. Here, we have investigated the molecular mechanism of catalysis and substrate recognition by *Haemophilus influenzae* YbaK using site-directed mutagenesis, enzymatic assays of isosteric substrates and functional group analogs, and computational modeling. These studies together with mass spectrometric characterization of the YbaK-catalyzed reaction products support a novel substrate-assisted mechanism of Cys-tRNA^{Pro} deacylation that prevents non-specific Pro-tRNA^{Pro} hydrolysis. Collectively, we propose that the INS and YbaK domains co-evolved distinct mechanisms involving steric exclusion and thiol-specific chemistry, respectively, to ensure accurate decoding of proline codons.

Aminoacyl-tRNA synthetases (aaRSs) play a pivotal role in the decoding of genetic information by catalyzing the esterification of cognate amino acids onto specific transfer RNAs (tRNAs) in a two-step reaction (1). The first step involves amino acid activation with ATP to form an aminoacyl-adenylate intermediate and

concomitant pyrophosphate release. The second step involves aminoacyl transfer to the cognate tRNA via a transesterification reaction. Although aaRSs display high substrate specificity, they often misactivate structurally similar amino acids. If left unchecked, these mistakes lead to errors in protein synthesis and accumulation of such errors can be deleterious to cells (2,3).

To ensure high fidelity in translation, aaRSs have evolved several proofreading mechanisms (4-7). In the first type of proofreading, misactivated aminoacyl-adenylates are enzymatically hydrolyzed, or selectively released from the active site followed by solvent hydrolysis, in a process termed “pre-transfer” editing. Another mechanism of proofreading known as “post-transfer” editing is generally believed to function via the so-called “double-sieve” mechanism (8). The model predicted that, whereas one active site could not completely discriminate Ile and Val, two separate active sites with distinct strategies for recognition could significantly enhance fidelity. The aminoacylation active site of the aaRS would act as a “coarse” sieve for adenylate synthesis, activating the cognate amino acid but also allowing, to a lesser extent, activation of isosteric or smaller amino acids that could fit into the amino acid binding pocket. The second “fine” sieve would selectively bind misactivated amino acids for editing, while excluding the original cognate amino acid. Thus, substrates synthesized in the first sieve, would be further screened by the second sieve to enhance fidelity. Subsequently, biochemical and structural data validated this steric exclusion mechanism for valyl-tRNA

synthetase (ValRS) and isoleucyl-tRNA synthetase (IleRS) (9,10). Indeed, members of both classes of synthetases are now known to possess a second active site spatially separated from the ancient catalytic core to carry out post-transfer editing. Structures of class I IleRS (10), leucyl-tRNA synthetase (LeuRS) (11), and ValRS (12) reveal the highly conserved connective peptide 1 domain that functions in editing. Class II alanyl-tRNA synthetase (AlaRS) (13,14), threonyl-tRNA synthetase (ThrRS) (15), prolyl-tRNA synthetase (ProRS) (16,17), and phenylalanyl-tRNA synthetase (18,19) also possess distinct domains for post-transfer editing. A recent study of AlaRS revealed an exception to the size-exclusion based double-sieve model of editing. In this case, a coordinated zinc ion in the editing site of AlaRS may help provide specificity for non-cognate serine, which is larger than cognate alanine (20,21). Insights into the relative contributions of pre- and post-transfer editing have also begun to emerge in several Class I and Class II synthetase systems (22-26).

Due to its unique side chain with special chemical properties, cysteine should be relatively easy for synthetases to discriminate. Similarly, proline is the only imino acid and would not be predicted to be especially problematic. Paradoxically, ProRSs from all domains of life confuse cysteine for proline (27,28). ProRSs also misactivate alanine and the majority of bacterial ProRSs possess an editing domain (INS) that can edit mischarged Ala-tRNA^{Pro} but not Cys-tRNA^{Pro} (17,29). We imagine that the smaller size of alanine relative to proline facilitates binding and catalysis by INS, whereas the editing domain rejects cysteine, which is very similar to proline in molecular volume (30). Consistent with this idea, the *Methanobacterium thermoautotrophicus* (31) and *Rhodospseudomonas palustris* (16) ProRS structures solved in complex with Cys- and Pro-sulfamoyl-adenylates showed that the aminoacylation active site of ProRS could accommodate both adenylates in a very similar manner. Thus, it is likely that a distinct post-transfer editing mechanism that does not rely on steric exclusion is needed to clear mischarged Cys-tRNA^{Pro}. Indeed, the latter is hydrolyzed by a freestanding domain known as YbaK, which is proposed to function in collaboration with ProRS in *trans* (29,32,33).

YbaK belongs to a larger protein superfamily that is widely distributed among all three kingdoms. Members of the YbaK superfamily share significant sequence and structural homology with the INS domain of bacterial ProRS (16,34-36). Interestingly, in contrast to YbaK, the freestanding PrdX domain within the YbaK superfamily possesses the same substrate specificity for Ala-tRNA^{Pro} as the INS domain (37). Freestanding editing domains have also been identified based on homology to the AlaRS and ThrRS editing domains. AlaXs generally display the same Ser- and Gly-tRNA^{Ala} editing specificity as the AlaRS protein (20,37-39), and ThrX possesses Ser-tRNA^{Thr} specificity similar to ThrRS (40). Thus, to date, YbaK is the only known editing domain homolog with distinct substrate specificity relative to the homologous synthetase domain.

Although the phenomenon of post-transfer editing in aaRSs is well established, relatively little is known about the detailed hydrolysis mechanism of freestanding editing proteins like YbaK at the molecular level (6,41-44). We were especially interested in understanding the basis for the unique Cys-tRNA specificity of YbaK and how discrimination of similar sized Pro-tRNA is achieved. The X-ray crystal structures of several members of the YbaK superfamily (PrdX, ProX, YbaK, and ProRS-INS) from a variety of organisms (protein data bank (PDB) codes 2DXA, 1DBX, 1VJF, 1WDV, 1VKI, 2CX5, 2ZOX, 2ZOK and 2J3L) have been solved (16,35,36). However, no structures of these proteins bound to post-transfer editing substrates are available to date. To understand the chemical basis of the distinct substrate specificities of these homologous editing domains, we investigated the mechanism of YbaK hydrolysis. Collectively, our experimental and computational data support a mechanism of catalysis that exploits the special side chain chemistry of cysteine.

METHODS

Materials—All amino acids and chemicals were purchased from Sigma unless otherwise noted. [³H]-Alanine (54 Ci/mmol), [³H]-proline (99 Ci/mmol), [³H]-serine (33 Ci/mmol) and [³²P]- α -ATP were from Amersham Biosciences and [³⁵S]-cysteine (1075 Ci/mmol) was from PerkinElmer Life Sciences.

Multiple sequence alignments—Multiple sequence alignments were performed using the ClustalW Multiple Sequence Re-alignment program (45).

Molecular modeling of CCA-Cys bound to H. influenzae YbaK—The crystal structure of monomeric *H. influenzae* YbaK was used as the starting structure (1DBX) (35). Missing residues 25-29 (NNQHF) in the flexible loop region were added using the template-based loop structure prediction server ArchPRED (46). The protonation states of the residues were calculated by PropKa (47). To relax the resulting structure and to sample the flexibility of the protein, 15 ns of MD simulation was performed in explicit solvent (TIP3P (48)) using AMBER 9 (49). Twenty-five snapshots of the protein structure from the resulting MD trajectory were extracted at equal time intervals and used for molecular docking. The structure of the 5'-CCA-Cys ligand was generated using the xleap module of AMBER 9. This ligand was docked onto the 25 structures of YbaK using AutoDock 4.0 (50). All of the ligand torsions were kept flexible, whereas the protein torsions were fixed. Each docking simulation involved generation of 200 different conformers, which were then clustered using a RMSD cutoff of 2.0 Å. Resulting clusters were manually inspected and the 5 docked structures most consistent with available mutagenesis data were chosen for further analysis. These structures were minimized using the ff99 force-field in AMBER 9, followed by 15 ns of MD simulation. The complex structure displaying the most stable trajectory was selected for further analysis. The final complex structure was subjected to 15 ns of MD to obtain time-averaged distance information and identify long-lived H-bonds. These analyses were performed using the ptraj module in AMBER 9.

Protein and tRNA preparation—All the proteins and tRNA substrates were prepared using published protocols as described in supplemental methods.

Aminoacylation Assays—To test YbaK's ability to prevent mischarging of beta-aminoalanine (β -Aa) onto tRNA^{Pro}, 1.5 μ M editing defective *E. coli* K279A ProRS was incubated with 10 μ M 3'-[³²P]-labeled tRNA^{Pro} and 150 mM β -Aa in 50 mM HEPES (pH 7.5), 4 mM ATP, 20 mM KCl, 50 mM dithiothreitol, 25 mM MgCl₂,

and 0.1 mg/ml BSA at 37 °C, in the absence or presence of 6 μ M YbaK. For each time point, 1.5 μ l of reaction mixture was quenched into 4.5 μ l of 200 mM NaOAc containing 0.4 unit/ μ l P1 nuclease at 4 °C. After digestion for 20 min at room temperature, 1 μ l of quenched mixture was spotted onto a polyethyleneimine (PEI)-cellulose TLC plate pre-run with water. Separation of β -Aa-AMP and AMP was accomplished by developing the TLC in 0.1 M ammonium acetate and 5% acetic acid. The radioactivity was analyzed by using a Typhoon phosphorimager and data were analyzed using Biorad Quantity One software. The fraction of free tRNA was determined from the ratio of AMP formed over the total AMP plus β -Aa-AMP.

Preparation of aminoacyl-tRNAs for use in deacylation assays was carried out as described (29). Briefly, [³H]-Ser-tRNA^{Pro} was prepared by incubating 2 μ M *E. coli* AlaRS-CQ and 8 μ M *E. coli* G1:C72/U70 tRNA^{Pro} in a reaction mixture containing [³H]-serine (9.1 μ M) and unlabeled serine (0.5 mM) in 50 mM HEPES (pH 7.5), 4 mM ATP, 20 mM KCl, 20 mM β -mercaptoethanol, 25 mM MgCl₂, and 0.1 mg/ml BSA. [³H]-Ala-tRNA^{Pro} was prepared using *E. coli* WT AlaRS and G1:C72/U70 tRNA^{Pro} in a similar manner. [³⁵S]-Cys-tRNA^{Pro} was prepared by incubating *E. coli* ProRS (8 μ M), *E. coli* tRNA^{Pro} (8 μ M) with [³⁵S]-cysteine (0.9 μ M) and unlabeled cysteine (50 μ M) in a reaction buffer containing 20 mM Tris-HCl (pH 7.5), 20 mM KCl, 10 mM MgCl₂, 25 mM dithiothreitol and 2 mM ATP as described previously. [³⁵S]-Cys-tRNA^{Cys} was prepared by incubating *E. coli* CysRS (30 nM) and *E. coli* tRNA^{Cys} (8 μ M) in the same reaction buffer. 3'-end modified (2'-dA76 or 3'-dA76) *E. coli* tRNA^{Cys} was charged with [³⁵S]-cysteine in a similar manner except a higher concentration of *E. coli* CysRS (5 μ M) was used. Sec-3'-[³²P]-tRNA^{Cys} was prepared by incubating *E. coli* CysRS (2 μ M) and *E. coli* tRNA^{Cys} (10 μ M) with freshly prepared 50 mM selenocysteine in a reaction buffer containing 20 mM Tris-HCl (pH 8.0), 20 mM KCl, 10 mM MgCl₂, 0.1 mg/ml BSA, 2 mM ATP and 50 mM tris-(2-carboxyethyl)phosphine (TCEP) in 0.1 M Tris-HCl buffer (pH 9.0) at 37 °C for 1 hr. A fresh solution of 140 mM selenocysteine was prepared immediately prior to use by dissolving seleno-L-cystine (Fluka) (11.7

mg, 0.035 mmol) in ~ 40 μ l of 0.2 N HCl. The diselenide bond was reduced in situ by addition of an equal volume of 0.2 M TCEP in 0.1 M Tris-HCl (pH 9.0) (51). The final volume (500 μ l) was made up with 0.1 M TCEP in 0.1 M Tris-HCl (pH 9.0), and the pH of the resulting solution was adjusted to ~7.5-8.0 with a few drops of 14 N NaOH. During ethanol precipitation of the Sec-tRNA, 50 μ l of 0.1 M TCEP solution was added to prevent auto-oxidation. 2-Abu (2-aminobutyric acid)-3'-[32 P]-tRNA^{Pro} was prepared by incubating 1.5 μ M *E. coli* K279A ProRS with 10 μ M 3'-[32 P]-labeled tRNA^{Pro} and 150 mM 2-Abu in 50 mM HEPES (pH 7.5), 4 mM ATP, 20 mM KCl, 50 mM dithiothreitol, 25 mM MgCl₂, and 0.1 mg/ml BSA at 37 °C.

Deacylation Assays—Deacylation assays were generally carried out at 37 °C according to published protocols. Reactions contained approximately 1.0 μ M G1:C72/U70 [3 H]-Ala-tRNA^{Pro}, 1.0 μ M G1:C72/U70 [3 H]-Ser-tRNA^{Pro}, 0.5 μ M [35 S]-Cys-tRNA^{Pro}, 1.0 μ M [3 H]-Pro-tRNA^{Pro}, 0.7 μ M [35 S]-Cys-2'-dA76-tRNA^{Cys} and 0.5 μ M [35 S]-Cys-3'-dA76-tRNA^{Cys}. Reactions were initiated with 0.5–1.0 μ M of WT or mutant YbaK, quenched and worked up as described (29). A background reaction was carried out in which buffer (0.15 M KPO₄, pH 7.0) was used to initiate the reaction for each substrate. For competition assays, various concentrations of G1:C72/U70 Ser-tRNA^{Pro} were mixed with 0.5 μ M [35 S]-Cys-tRNA^{Pro} and reactions were initiated by addition of 0.1 μ M YbaK. In other competition assays, Sec-tRNA^{Cys}, Cys-2'-dA76-tRNA^{Cys} or Cys-tRNA^{Cys} (~6-8 μ M each) were mixed with 0.5 μ M [35 S]-Cys-tRNA^{Cys} and reactions were initiated by addition of 0.5 μ M YbaK. 2-Abu-[32 P]-tRNA^{Pro}, Sec-[32 P]-tRNA^{Cys} and Cys-[32 P]-tRNA^{Cys} deacylation assays contained 1 μ M of each tRNA and 0.5-5 μ M YbaK. Reactions were quenched by adding 0.4 unit/ μ l P1 nuclease in 200 mM NaOAc and the deacylation level was analyzed using PEI-cellulose TLC, as previously described (52). The fraction of aminoacyl-tRNA remaining was plotted as a function of time and fitted to a single-exponential equation to obtain k_{obs} . All assays were carried out in triplicate. In some cases, analysis of reaction products was performed by ESI-MS and LC/MS as described in the supplemental methods.

RESULTS

Sequence analysis of the YbaK superfamily—Freestanding domains with homology to the ProRS editing domain have been identified across a variety of species and can be grouped together to constitute a “YbaK superfamily”. In addition to the INS domain of bacterial ProRS, phylogenetic analysis using available sequences in the PDB indicates that members of this superfamily include at least 5 distinct freestanding protein domains designated YbaK, YeaK, ProX, PrdX and PA2301. Despite their relatively low sequence identity, these proteins possess high structural homology (16,34,35). Interestingly, members of the YbaK superfamily investigated to date show distinct substrate specificities. Whereas the INS domain specifically hydrolyzes Ala-tRNA^{Pro}, bacterial YbaK possesses post-transfer editing activity against Cys-tRNA *in vitro* and *in vivo* (29,32). In contrast, *Clostridium sticklandii* PrdX has been reported to display Ala-tRNA^{Pro} deacylation specificity (37). The chemical basis for the altered substrate specificity within the YbaK superfamily is not understood.

To begin to address this question, a multiple sequence alignment of YbaK superfamily members with known function, including YbaK, the INS domain of ProRS, and PrdX was performed using the ClustalW Multiple Sequence Re-alignment program (Fig. 1). A separate alignment of the 105-member YbaK subfamily was also carried out (supplemental Fig. 1). As noted previously (35), a Lys residue (Lys46 in *H. influenzae* YbaK) and a GXXX motif are almost universally conserved in the YbaK superfamily (Fig. 1). The GXXX motif, which resembles a common sequence element in serine-proteases (35) and D-Tyr-tRNA^{Tyr} deacylases (53), forms part of a flexible loop in the X-ray crystal structures of *E. faecalis* ProRS (16) and *H. influenzae* YbaK (35). In addition, several other highly conserved residues in the YbaK subfamily include surface-exposed lysines and glycines in the flexible random coil regions of YbaK.

Computational modeling of CCA-Cys bound to *H. influenzae* YbaK—There are presently no available structures of post-transfer editing substrates or substrate analogs bound to the active site of *H. influenzae* YbaK or its homologs. To begin to probe the chemical basis of substrate

recognition and the mechanism of Cys-tRNA^{Pro} hydrolysis by YbaK, we used computational approaches to generate a docking model of a 5'-CCA-Cys substrate mimic in the *H. influenzae* YbaK active site. The model of the YbaK-CCA-Cys complex was generated using a judicious combination of molecular docking (AUTODOCK 4) and molecular dynamics (MD) simulations (AMBER 9), as described in the methods section. Stability of the complex, distances between important functional groups, and the occupancy (life-times) of the H-bonds were assessed by analyzing the MD trajectory of the complex structure.

The modeled complex shows an extended active site binding pocket that accommodates the three nucleotides of the ligand (Fig. 2A). The cysteine moiety binds in a deep cleft and interacts directly with several functionally important residues identified by the mutagenesis studies described below (Fig. 2B, purple residues). The Phe29 of the NNQHF loop (Fig. 2B, yellow), which is missing in the X-ray structure of *H. influenzae* YbaK and was therefore built into the model, is positioned on top of the bound ligand and presumably stabilizes the complex. The O1P and O2P oxygen atoms of the A76 phosphate form H-bonds with the Lys46 amine with 96.8% and 65.6% occupancy, respectively (Fig. 3A). These interactions are consistent with the critical nature of this lysine residue for activity (29), as well as with the X-ray structure of apo-*E. faecalis* ProRS, where the equivalent lysine is bound to a solvent SO₄²⁻ moiety (16). Thus, the highly conserved lysine in the YbaK superfamily appears to play a general role in stabilizing the bound conformation of the tRNA in the active site. The C75 phosphate also forms strong H-bonds (greater than 90% occupancy) with the protein. The O1P oxygen forms a H-bond with the side chain NδH of His28, whereas the O2P oxygen forms two H-bonds with the backbone NH groups of Phe29 and Gly30 (Fig. 3B).

One of the most stable binding interactions between YbaK and CCA-Cys involves the adenine base of A76. Our analysis showed three long-lived H-bonds, one between the N7 of A76 and the Leu49 backbone NH, and two between the N6 hydrogens of A76 and the backbone carbonyls of Leu49 and Ala87 (Fig. 3C). These interactions

appear to play a critical role in properly orienting the substrate in the active site.

The orientation of the cysteine was highly stable over the course of the MD simulation. Two H-bonds form between the amine of the substrate cysteine moiety and the side chain oxygen atoms of Tyr20 and Ser129 (Fig. 3D). The substrate amine group also forms H-bonds with backbone carbonyls of the KRG loop (Lys132, Arg133, Gly134; Fig. 2B, cyan). The carbonyl oxygen of the cysteine moiety points to the center of a cluster of hydroxyl groups belonging to A76 (2'-OH), Thr47, and Ser129, with average distances (to the O of the hydroxyl groups) of 3.3, 2.9, and 3.6 Å, respectively (Fig. 3D). While the modeling results support close interactions between the carbonyl and amine groups of the substrate amino acid with the YbaK active site, the position of the side chain thiol, which lies in a rather large active site pocket, is notable for its *lack* of direct interaction with protein residues. Three polar residues, Ser44, Thr66, and Ser136, in this active site pocket surround the thiol group, with their side chain hydroxyl oxygen atoms located 4.1, 5.3, and 4.3 Å away from the thiol proton, respectively.

Cys-tRNA^{Pro} deacylation by WT and mutant H. influenzae YbaK—To probe the role of conserved positions in the YbaK subfamily, as well as residues in the substrate binding pocket based on the computational modeling, 22 residues were individually mutated to alanine. These were chosen based on the sequence alignments described above. Residues in four categories were chosen for alanine-scanning mutagenesis: (1) residues highly conserved within the entire YbaK superfamily (Lys46, Gly101; numbering based on *H. influenzae* YbaK); (2) residues highly conserved in the YbaK subfamily only (Thr47, Thr96, Gly97, Tyr98, Ser129, Gly131, and Gly134); (3) residues only partially conserved in the YbaK subfamily (Tyr20, Phe29, Gln108, Thr114, Asn117, Tyr127, Lys132, and Arg133); and (4) residues not conserved but close to the predicted substrate-binding pocket based on modeling studies (Asp31, Glu32, Ser44, Thr66, and Ser136).

Initial assays were performed using 1 μM WT or mutant *H. influenzae* YbaK and 1 μM *E. coli* Cys-tRNA^{Pro}, and relative deacylation activity was calculated based on the level of deacylation at 30 min (supplemental Fig. 2). Most of the mutants

tested in these assays (D31A, E32A, S44A, T66V, T96A, G97A, Q108A, T114A, N117A, Y127A, K132A, R133A, G134A and S136A) displayed robust deacylation activity ($\geq 50\%$ of WT YbaK). For the mutants that showed lower than 50% activity, a more detailed kinetic analysis was performed, wherein the rate of deacylation was measured as a function of time (k_{obs}) and compared to that of WT YbaK (Table 1). In addition, some positions close to the substrate binding pocket were probed in more detail, and in a few cases, mutants to non-alanine residues were made and tested.

Previously, we showed that Lys46 of *H. influenzae* YbaK is critical for Cys-tRNA^{Pro} deacylation activity (29). The kinetic analysis performed here showed a 66-fold decrease in deacylation efficiency for the K46A variant relative to WT YbaK (Table 1). To gain further insights into the role of this key residue, K46I and K46R variants were tested. Both the hydrophobic mutation (K46I) and the conservative mutation (K48R) significantly reduced hydrolysis activity (38- and 44-fold, respectively). Due to its critical nature, the Lys46 residue was earlier suggested to play a catalytic role in Cys-tRNA^{Pro} deacylation (29). In contrast, our modeling suggests that Lys46 is involved in binding tRNA^{Pro} and positioning the 3' end into the substrate binding pocket (Fig. 3A). This second hypothesis is supported by the mutagenesis data showing sensitivity to even a conservative arginine substitution. A similar role for the corresponding Lys279 residue has been postulated for Ala-tRNA^{Pro} hydrolysis by the INS domain of *E. coli* ProRS (16). We also probed Gly101, which is a part of the GXXXP motif proposed to be analogous to the “oxyanion hole” found in serine proteases and D-Tyr-tRNA^{Tyr} deacylases (35,53). The G101A mutation results in a 36-fold reduction in deacylation activity, consistent with a possible role in stabilizing the oxyanionic tetrahedral intermediate generated during ester bond hydrolysis.

In addition to Lys46 and Gly101, which are almost universally conserved in the YbaK superfamily (Fig. 1 and supplemental Fig. 1), several other highly conserved residues in the YbaK subfamily were probed in more detail. Alanine substitutions of Thr47, Ser129, Gly131 and Gly134 resulted in 6- to 28-fold decreases in deacylation efficiency. Upon mutation to alanine,

semi-conserved aromatic residues in the YbaK subfamily, Tyr20 and Phe29, displayed 45- and 29-fold decreases in activity, respectively. Although Ser44, Thr66, and Ser136 are not conserved in the YbaK subfamily, these residues were selected for mutation due to their location proximal to the substrate-binding pocket. Whereas a S136A substitution resulted in 4-fold reduced activity, S136H displayed a 16-fold reduction. The greater effect of histidine substitution implies that YbaK catalysis is sensitive to the substrate binding pocket size or polarity. Alanine and valine substitutions of hydrophilic Ser44 and Thr66 side chains, respectively, resulted in small (≤ 2.1 -fold) reductions in activity compared to WT YbaK (Table 1). In summary, the mutagenesis study provided experimental support for the computationally derived docking model, identifying functionally important interactions in and around the substrate binding pocket (Fig. 2B).

Substrate specificity and role of substrate functional groups in YbaK catalysis—YbaK catalyzes hydrolysis of Cys-tRNA and does not show activity against isosteric substrates Ala-tRNA^{Pro}, Gly-tRNA^{Ala}, and Ser-tRNA^{Ala} (Fig. 4A) using 1 μM of protein (29). At very high enzyme concentration (21 μM), weak hydrolysis of these substrates was observed (29). To determine whether any of the YbaK mutants display altered substrate specificity, we tested the ability of the majority of the YbaK variants to hydrolyze non-specific substrates Ala-, Ser-, and Pro-tRNA^{Pro}. In all cases, the substrate specificity of the mutants was similar to that of WT YbaK, i.e., none of the mutants displayed significantly enhanced ability to hydrolyze the non-specific substrates even in the presence of very high concentrations of mutant proteins (21 μM) (supplemental Table 1).

We also tested two non-natural amino acids, 2-Abu and β -Aa (Fig. 4A) for hydrolysis by WT YbaK. These substrates are isosteres of cysteine where the thiol group is replaced by either a methyl or amine group, respectively. As shown in Figure 4B, 2-Abu-tRNA^{Pro} was not a substrate for deacylation by YbaK (0.5 μM). In the case of β -Aa, sufficient quantities of mischarged tRNA could not be readily generated for deacylation assays; however, a mischarging assay conducted in the presence and absence of YbaK is consistent with a lack of hydrolysis activity (Fig. 4C). Taken

together, our data suggest that the substrate cysteine thiol side chain is required for catalysis by YbaK.

Although Ser-tRNA is not a substrate for YbaK deacylation, we wanted to test whether Ser-tRNA binds to the same active site as Cys-tRNA. To address this question, Cys-tRNA^{Pro} deacylation assays were performed in the presence of various concentrations of Ser-tRNA^{Pro} (Fig. 4D). These studies showed that YbaK deacylation of Cys-tRNA^{Pro} was inhibited in the presence of Ser-tRNA^{Pro} with ~65% inhibition observed at 1 μ M Ser-tRNA^{Pro}. These results support the conclusion that cysteine and serine occupy the same active site, but only Cys-tRNA is a substrate for YbaK deacylation, suggesting a critical role for the cysteine thiol group in catalysis.

We next wanted to establish whether the specificity for cysteine over serine was conferred by the presence of a zinc ion in the active site. A similar role for zinc has been demonstrated in the case of cysteinyl-tRNA synthetase (CysRS) (54). Atomic absorption spectroscopic analysis revealed that purified *H. influenzae* YbaK did not contain bound zinc ions, as expected from the available *H. influenzae* YbaK crystal structure (35). Nevertheless, we tested the effect of zinc on YbaK deacylation by supplementing the reaction buffer with 5 mM ZnCl₂. The results showed that zinc addition had no effect on deacylation activity (supplemental Fig. 3). Furthermore, EDTA treatment to chelate any residual zinc following protein purification also failed to alter catalysis by YbaK (supplemental Fig. 3).

Previous studies have shown that the *cis*-hydroxyl groups of the terminal A76 of tRNA are critical for deacylation by aaRSs (44,55-57). To examine the role of the 3'-terminal hydroxyl groups in YbaK deacylation, Cys-tRNA analogs lacking either the 2'- or 3'- hydroxyl group were prepared. Due to poor levels of cysteine charging onto dA76 tRNA^{Pro} variants by ProRS, dA76 tRNA^{Cys} variants were used for this study. CysRS has previously been shown to aminoacylate cysteine on 2'-dA76- or 3'-dA76-tRNA^{Cys} (58). As shown in Figure 4E, neither the 2'- nor the 3'-dA76 Cys-tRNA^{Cys} variant was hydrolyzed by YbaK, whereas WT Cys-tRNA^{Cys} was readily deacylated. Based on our level of detection, we estimate that the single deoxy substitutions result in at least a 100-fold decrease in deacylation efficiency. We

showed that Cys-2'-dA76-tRNA^{Cys} serves as a competitive inhibitor of Cys-tRNA^{Cys} deacylation by YbaK (Fig. 4E, inset), indicating that binding is not significantly affected by the deoxy substitution. These data suggest that the hydroxyl group proximal to the site of esterification plays a critical role in catalysis by YbaK.

Role of Cysteine thiol group in hydrolysis by YbaK—A previous study demonstrated that *E. coli* CysRS displays weak hydrolysis of Cys-tRNA^{Cys} in the aminoacylation site and suggested that this may occur via cysteine-thiolactone formation (59). To test this as a possible mechanism for YbaK deacylation, we analyzed the YbaK-catalyzed [³⁵S]-Cys-tRNA^{Pro} deacylation products using cellulose TLC. A major species (Fig. 5A, lane 3-5, product) is observed with an R_f value that is distinct from that of free cysteine (Fig. 5A, lane 6). In the absence of YbaK, this compound was not detected by TLC (Fig. 5A, lane 1 and 2), suggesting that this compound is generated during YbaK catalysis. We also showed that the major YbaK product does not co-migrate with cysteine (Fig. 5A, lane 7).

To identify the product formed upon YbaK catalysis, we analyzed the crude reaction mixture using high-resolution electrospray ionization mass spectrometry (ESI-MS) with methanol as a carrier solvent (supplemental Fig. 4). The major species in the spectrum was observed at 158.0246 amu, and was assigned as the Na⁺ adduct of cysteine methyl ester (theoretical m/z = 158.0246). This assignment was further validated with an authentic sample of cysteine methyl ester. We propose that the cysteine methyl ester is produced by methanol-activated transesterification of a thiolactone intermediate formed upon YbaK-catalyzed hydrolysis of Cys-tRNA (Fig. 6B). A similar esterification reaction between free cysteine and methanol is kinetically less feasible and thus, not observed (Fig. 6A). Reaction mixtures were also analyzed by tandem LC/MS. In the presence of YbaK, a distinct peak was observed at 3.5 min that is well separated from free cysteine at 1 min (Fig. 5B), and this major peak was confirmed to be the cysteine methyl ester by MS/MS analysis (M+H=136). YbaK-independent transesterification of Cys-tRNA^{Pro} by methanol can be ruled out since only free cysteine is observed in the absence of YbaK (Fig. 5B). In a control reaction, free cysteine was analyzed in methanol solution, and no

cysteine methyl ester peak was detected. These data support the conclusion that YbaK-catalyzed Cys-tRNA^{Pro} hydrolysis proceeds via a cysteine-thiolactone intermediate.

Based on the chemical similarity between cysteine and selenocysteine, we hypothesized that substitution of the side chain sulfur for a selenium atom would support deacylation by YbaK. To test this hypothesis, we mis-acylated tRNA^{Cys} with selenocysteine using CysRS and measured the rates of deacylation by YbaK. YbaK deacylates Sec-tRNA^{Cys}, albeit with an ~10-fold reduced rate relative to Cys-tRNA^{Cys} (Fig. 7A). Nevertheless, these results further support the mechanism shown in Figure 6B.

DISCUSSION

Several biochemical, computational, and X-ray crystallographic studies examining post-transfer editing mechanisms of aaRSs have proposed water-mediated cleavage of the aminoacyl-tRNA ester bond (Fig. 6A) (43,44,55-57). Class I LeuRS and IleRS and class II ThrRS and PheRS activate water molecules via interaction with conserved residues in their editing active sites. In addition, editing often occurs via substrate-assisted catalysis involving the hydroxyl groups of the A76 ribose on tRNA (44,56,57). In all of these systems, a double-sieve mechanism is used, involving steric exclusion of the cognate aminoacyl-tRNA from the editing domain. In contrast, our data are consistent with an alternate mechanism that exploits the unique chemistry of the thiol side chain.

The thiol group of free cysteine is a strong nucleophile with a pK_a value of 8.3. Furthermore, the pK_a of cysteine in the active site of a protein may be suppressed by as much as 2 units when close to polar or charged residues (60). In our model of *H. influenzae* YbaK, the substrate cysteine thiol is located close to several non-conserved polar residues (Ser44, Thr66, and Ser136) (Fig. 8). In *E. coli* YbaK, Ser136 is replaced by a charged aspartate residue. As expected, mutation of these non-conserved residues is not critical for hydrolysis. Nevertheless, the environment of the active site may lower the cysteine pK_a resulting in thiolate-attack of the carbonyl center and formation of a four-membered thiolactone intermediate (Fig. 6B).

Interestingly, the average side chain dihedral χ_1 of cysteine in our model is 54.2°, which brings the thiol sulfur in close proximity to the carbonyl carbon (3.3 Å) at an angle of 105°, making it facile for nucleophilic attack. Cyclization would be less favorable for a serine substrate because of the higher pK_a (~13) of its hydroxyl side chain. In addition, a four-membered lactone would be highly constrained due to the shorter C-O bond length. On the other hand, selenocysteine was found to be a substrate for YbaK. Given the lower pK_a of the selenol group (~5.2), the apparent 10-fold reduction in rate for the Sec-tRNA^{Cys} substrate is somewhat surprising. Computational studies showed that the selenolactone ring strain is actually *lower* than that of the thiolactone (supplemental Table 3), supporting the prediction that selenocysteine should be a better substrate than cysteine. In addition, using a competition assay, we showed that ~6 μM Cys-tRNA^{Cys} or Sec-tRNA^{Cys} both competitively inhibit YbaK deacylation of Cys-tRNA^{Cys} (Fig. 7B), suggesting there is not a significant tRNA binding defect. Thus, even though global tRNA binding is not affected, we hypothesize that the larger selenocysteine group may perturb the active site leading to slight destabilization of the transition state and decrease the rate of catalysis.

The formation of cyclized adducts in the active sites of aaRSs is not unprecedented. Studies of aaRSs that utilize amino acids featuring nucleophilic side chains as substrates have demonstrated that in addition to Cys-tRNA^{Cys} hydrolysis by CysRS (59), adenylates of homocysteine and ornithine can be hydrolyzed in the activation sites of MetRS, and LysRS, respectively (59,61,62). The latter reactions have been proposed to occur via cyclization mechanisms that result in the formation of homocysteine thiolactone and ornithine lactam.

In addition to the substrate thiol, the 2'-hydroxyl group of A76 is also crucial for YbaK-catalyzed deacylation of Cys-tRNA. This supports our proposed mechanism that YbaK functions by binding the substrate in an orientation that facilitates cyclization of the substrate cysteine while excluding water molecules from the active site. It is noteworthy that all the functionally important conserved residues in the YbaK subfamily examined here appear to either play a structural role (Gly131 and Gly134), or are

involved in the stabilization of the aminoacyl-tRNA (Lys46 and Ser129) or the oxyanionic reaction intermediate (Thr47 and Gly101) (Fig. 8). Although none of these residues provide specificity for cysteine per se, this is consistent with the proposed catalytic role of substrate cysteine. Our proposed mechanism is also consistent with the observation that none of the active site mutations result in a complete loss in enzymatic activity. The most deleterious mutation occurs at a residue (Lys46) that is present in all members of the YbaK superfamily (Fig. 1) and which has been proposed to play a general role in positioning the catalytically competent orientation of the substrate in the active site of the enzyme (Fig. 8).

Editing defects in AlaRS are toxic to bacteria and linked to neurodegeneration in mice that harbor a gene encoding the mutant synthetase (2,13). Although AlaRSs edit both Gly- and Ser-tRNA^{Ala}, free-standing AlaXps co-evolved as a second check-point to ensure editing of Ser-tRNA^{Ala}, which poses a greater challenge than glycine (38,63). Although, even mild editing defects have been linked to serious pathology in the mouse (2), the presence of ~10% mismatched protein is not detrimental to *E. coli* (64). Thus, different organisms and cellular environments display different requirements with respect to error rate tolerance.

The widespread occurrence of a Cys-tRNA deacylase in bacteria (Fig. 1) is consistent with the importance of proline and cysteine residues for protein structure and function. Proline to cysteine mutations can potentially result in drastic consequences as a result of protein misfolding or disruption of regulatory mechanisms in the cell. The distinct mechanism of YbaK catalysis offers insights into the evolutionary pressure to evolve and maintain a separate *trans*-editing domain to clear mistakes made by ProRS. During aminoacylation, ProRS cannot effectively

discriminate between proline (90 Å³) and cysteine (86 Å³) due to their similar Van der Waals volumes (30). This is also evident from the overlapping orientations of the corresponding aminoacyl-adenylates bound in the amino acid activation site of ProRS (16,31). The INS domain of ProRS (and the homologous PrdX domain (32,37), see Fig. 1) selectively clears Ala-tRNA^{Pro} based on the double-sieve mechanism of editing that functions via steric exclusion of proline. A model of the *E. faecalis* INS·CCA-Ala complex (supplemental Fig. 5) generated by homology modeling using our final YbaK·CCA-Cys complex model as a starting structure, predicts that the methyl side chain of substrate alanine binds in a small hydrophobic pocket formed by conserved residues Ile263 and Val266. This pocket is too small to accommodate larger amino acids proline and cysteine without disrupting active site geometry (S. K., M. D., C. H., and K. M.-F., unpublished data). Had the INS domain evolved a larger binding pocket to accommodate and edit cysteine in addition to alanine, it would have been more challenging to discriminate against cognate proline.

In addition, computational studies showed that CCA-Pro can bind YbaK with an orientation similar to that of CCA-Cys, albeit with somewhat lower affinity (supplemental results and Table 2). Therefore, if YbaK had evolved to clear cysteine via a general water-mediated mechanism rather than via thiol-specific chemistry, cognate proline would also be hydrolyzed. We propose that the INS domain and YbaK co-evolved distinct mechanisms involving the use of steric exclusion and thiol-specific chemistry, respectively, to prevent non-specific hydrolysis of correctly charged Pro-tRNA^{Pro}. In this manner, the fine sieve of the ProRS INS domain and the chemical sieve of YbaK collaborate to ensure accurate decoding of proline codons.

REFERENCES

1. Ibba, M., and Söll, D. (2000) *Annu. Rev. Biochem.* **69**, 617-650
2. Lee, J. W., Beebe, K., Nangle, L. A., Jang, J., Longo-Guess, C. M., Cook, S. A., Davisson, M. T., Sundberg, J. P., Schimmel, P., and Ackerman, S. L. (2006) *Nature* **443**, 50-55
3. Nangle, L. A., Motta, C. M., and Schimmel, P. (2006) *Chem. Biol.* **13**, 1091-1100
4. Jakubowski, H., and Goldman, E. (1992) *Microbiol. Mol. Biol. Rev.* **56**, 412-429
5. Hendrickson, T. L., de Crécy-Lagard, V., and Schimmel, P. (2004) *Annu. Rev. Biochem.* **73**, 147-176
6. Mascarenhas, A. P., Martinis, S. A., An, S., Rosen, A. E., and Musier-Forsyth, K. (2008) Fidelity mechanisms of the aminoacyl-tRNA synthetases. in *Protein Engineering* (RajBhandary, U. L., and Koehler, C. eds.), Springer-Verlag, New York. pp 153-200
7. Ling, J., Reynolds, N., and Ibba, M. (2009) *Annu. Rev. Microbiol.* **63**, 61-78
8. Fersht, A. R. (1977) *Enzyme Structure and Mechanism*, Freeman, San Francisco
9. Fersht, A. R., and Dingwall, C. (1979) *Biochemistry* **18**, 2627-2631
10. Nureki, O., Vassilyev, D. G., Tateno, M., Shimada, A., Nakama, T., Fukai, S., Konno, M., Hendrickson, T. L., Schimmel, P., and Yokoyama, S. (1998) *Science* **280**, 578-582
11. Lincecum, T. L., Jr., Tukalo, M., Yaremchuk, A., Mursinna, R. S., Williams, A. M., Sproat, B. S., Van Den Eynde, W., Link, A., Van Calenbergh, S., Grotli, M., Martinis, S. A., and Cusack, S. (2003) *Mol. Cell* **11**, 951-963
12. Fukai, S., Nureki, O., Sekine, S., Shimada, A., Tao, J., Vassilyev, D. G., and Yokoyama, S. (2000) *Cell* **103**, 793-803
13. Beebe, K., Ribas De Pouplana, L., and Schimmel, P. (2003) *EMBO J.* **22**, 668-675
14. Naganuma, M., Sekine, S., Fukunaga, R., and Yokoyama, S. (2009) *Proc. Natl. Acad. Sci. USA* **106**, 8489-8494
15. Dock-Bregeon, A., Sankaranarayanan, R., Romby, P., Caillet, J., Springer, M., Rees, B., Francklyn, C. S., Ehresmann, C., and Moras, D. (2000) *Cell* **103**, 877-884
16. Crepin, T., Yaremchuk, A., Tukalo, M., and Cusack, S. (2006) *Structure* **14**, 1511-1525
17. Beuning, P. J., and Musier-Forsyth, K. (2000) *Proc. Natl. Acad. Sci. USA* **97**, 8916-8920
18. Kotik-Kogan, O., Moor, N., Tworowski, D., and Safro, M. (2005) *Structure* **13**, 1799-1807
19. Roy, H., Ling, J., Irnov, M., and Ibba, M. (2004) *EMBO J.* **23**, 4639-4648
20. Sokabe, M., Okada, A., Yao, M., Nakashima, T., and Tanaka, I. (2005) *Proc. Natl. Acad. Sci. USA* **102**, 11669-11674
21. Sokabe, M., Ose, T., Nakamura, A., Tokunaga, K., Nureki, O., Yao, M., and Tanaka, I. (2009) *Proc. Natl. Acad. Sci. USA* **106**, 11028-11033
22. Boniecki, M. T., Vu, M. T., Betha, A. K., and Martinis, S. A. (2008) *Proc. Natl. Acad. Sci. USA* **105**, 19223-19228
23. Dulic, M., Cvetic, N., Perona, J.J., Gruic-Sovulj, I. (2010) *J. Biol. Chem.* **285**, 23799-23809
24. Splan, K. E., Ignatov, M. E., and Musier-Forsyth, K. (2008) *J. Biol. Chem.* **283**, 7128-7134
25. Yadavalli, S. S., Musier-Forsyth, K., and Ibba, M. (2008) *Proc. Natl. Acad. Sci. USA* **105**, 19031-19032
26. Minajigi, A., and Francklyn, C. S. (2010) *J. Biol. Chem.* **285**, 23810-23817
27. Beuning, P. J., and Musier-Forsyth, K. (2001) *J. Biol. Chem.* **276**, 30779-30785
28. Ahel, I., Stathopoulos, C., Ambrogelly, A., Sauerwald, A., Toogood, H., Hartsch, T., and Söll, D. (2002) *J. Biol. Chem.* **277**, 34743-34748
29. An, S., and Musier-Forsyth, K. (2004) *J. Biol. Chem.* **279**, 42359-42362
30. Creighton, T. E. (1996) *Proteins Structure and Molecular Properties*, Freeman, New York

31. Kamtekar, S., Kennedy, W. D., Wang, J., Stathopoulos, C., Söll, D., and Steitz, T. A. (2003) *Proc. Natl. Acad. Sci. USA* **100**, 1673-1678
32. Ruan, B., and Söll, D. (2005) *J. Biol. Chem.* **280**, 25887-25891
33. An, S., and Musier-Forsyth, K. (2005) *J. Biol. Chem.* **280**, 34465-34472
34. Wolf, Y. I., Aravind, L., Grishin, N. V., and Koonin, E. V. (1999) *Genome Res.* **9**, 689-710
35. Zhang, H., Huang, K., Li, Z., Banerjee, L., Fisher, K. E., Grishin, N. V., Eisenstein, E., and Herzberg, O. (2000) *Proteins: Struct. Funct. Bioinform.* **40**, 86-97
36. Murayama, K., Kato-Murayama, M., Katsura, K., Uchikubo-Kamo, T., Yamaguchi-Hirafuji, M., Kawazoe, M., Akasaka, R., Hanawa-Suetsugu, K., Hori-Takemoto, C., Terada, T., Shirouzu, M., and Yokoyama, S. (2005) *Acta Crystallogr. Sect. F Struct. Biol. Cryst. Commun.* **61**, 26-29
37. Ahel, I., Korencic, D., Ibba, M., and Söll, D. (2003) *Proc. Natl. Acad. Sci. USA* **100**, 15422-15427
38. Beebe, K., Mock, M., Merriman, E., and Schimmel, P. (2008) *Nature* **451**, 90-93
39. Guo, M., Chong, Y. E., Shapiro, R., Beebe, K., Yang, X. L., and Schimmel, P. (2009) *Nature* **462**, 808-812
40. Korencic, D., Ahel, I., Schelert, J., Sacher, M., Ruan, B., Stathopoulos, C., Blum, P., Ibba, M., and Söll, D. (2004) *Proc. Natl. Acad. Sci. USA* **101**, 10260-10265
41. Hendrickson, T. L., Nomanbhoy, T. K., de Crécy-Lagard, V., Fukai, S., Nureki, O., Yokoyama, S., and Schimmel, P. (2002) *Mol. Cell* **9**, 353-362
42. Wong, F. C., Beuning, P. J., Nagan, M., Shiba, K., and Musier-Forsyth, K. (2002) *Biochemistry* **41**, 7108-7115
43. Dock-Bregeon, A. C., Rees, B., Torres-Larios, A., Bey, G., Caillet, J., and Moras, D. (2004) *Mol. Cell* **16**, 375-386
44. Ling, J., Roy, H., and Ibba, M. (2007) *Proc. Natl. Acad. Sci. USA* **104**, 72-77
45. Thompson, J. D., Higgins, D. G., and Gibson, T. J. (1994) *Nucleic Acids Res.* **22**, 4673-4680
46. Fernandez-Fuentes, N., Zhai, J., and Fiser, A. (2006) *Nucleic Acids Res.* **34**, W173-176
47. Jensen, J. H., Li, H., Robertson, A. D., and Molina, P. A. (2005) *J. Phys. Chem. A* **109**, 6634-6643
48. Jorgensen, W. L., Chandrasekhar, J., Madura, J. D., Impey, R. W., and Klein, M. L. (1983) *J. Chem. Phys.* **79**, 926-935
49. Case, D. A., Darden, T.A., Cheatham, T.E.III, Simmerling, C.L., Wang, J., Duke, R.E., Luo, R., Merz, K.M., Pearlman, D.A., Crowley, M., Walker, R.C., Zhang, W., Wang, B., Hayik, S., Roitberg, A., Seabra, G., Wong, K.F., Paesani, F., Wu, X., Brozell, S., Tsui, V., Gohlke, H., Yang, L., Tan, C., Mongan, J., Hornak, V., Cui, G., Beroza, P., Matthews, D.H., Schafmeister, C., Ross, W.S. and Kollman, P.A. (2006) AMBER 9. University of California, San Francisco
50. Huey, R., Morris, G. M., Olson, A. J., and Goodsell, D. S. (2007) *J. Comput. Chem.* **28**, 1145-1152
51. Hondal, R. J., Nilsson, B. L., and Raines, R. T. (2001) *J. Am. Chem. Soc.* **123**, 5140-5141
52. Wolfson, A. D., and Uhlenbeck, O. C. (2002) *Proc. Natl. Acad. Sci. USA* **99**, 5965-5970
53. Lim, K., Tempczyk, A., Bonander, N., Toedt, J., Howard, A., Eisenstein, E., and Herzberg, O. (2003) *J. Biol. Chem.* **278**, 13496-13502
54. Newberry, K. J., Hou, Y. M., and Perona, J. J. (2002) *EMBO J.* **21**, 2778-2787
55. Igloi, G. L., von der Haar, F., and Cramer, F. (1977) *Biochemistry* **16**, 1696-1702
56. Nordin, B. E., and Schimmel, P. (2002) *J. Biol. Chem.* **277**, 20510-20517
57. Hagiwara, Y., Nureki, O., and Tateno, M. (2009) *FEBS Lett.* **583**, 1901-1908
58. Shitivelband, S., and Hou, Y. M. (2005) *J. Mol. Biol.* **348**, 513-521
59. Jakubowski, H. (1994) *Nucleic Acids Res.* **22**, 1155-1160
60. Witt, A. C., Lakshminarasimhan, M., Remington, B. C., Hasim, S., Pozharski, E., and Wilson, M. A. (2008) *Biochemistry* **47**, 7430-7440
61. Jakubowski, H. (1990) *Proc. Natl. Acad. Sci. USA* **87**, 4504-4508
62. Jakubowski, H. (1999) *Biochemistry* **38**, 8088-8093

63. Chong, Y. E., Yang, X. L., and Schimmel, P. (2008) *J. Biol. Chem.* **283**, 30073-30078
64. Ruan, B., Palioura, S., Sabina, J., Marvin-Guy, L., Kochhar, S., Larossa, R. A., and Söll, D. (2008) *Proc. Natl. Acad. Sci. USA* **105**, 16502-16507

FOOTNOTES

We thank Dr. M. Ignatov (The Ohio State University) for help with sequence alignments and Drs. T. R. Hoyer, J. Jeon and A. E. May (University of Minnesota) for their assistance in ESI-MS and LC/MS analyses. We thank Dr. Michael Ibbá (The Ohio State University) for helpful discussion and critical reading of the manuscript. The plasmid encoding *E. coli* tRNA^{NTase} was provided by Dr. P. Schimmel (The Scripps Research Institute). Generous computational resources were provided by the Ohio Supercomputer Center. This work was funded by NIH grant GM049928.

Abbreviations: aaRS, aminoacyl-tRNA synthetase; ProRS, prolyl-tRNA synthetase; AlaRS, alanyl-tRNA synthetase; IleRS, isoleucyl-tRNA synthetase; ThrRS, threonyl-tRNA synthetase; ValRS, valyl-tRNA synthetase; CysRS, cysteinyl-tRNA synthetase; INS, editing domain of bacterial ProRS; tRNA, transfer RNA; MD, molecular dynamics; BSA, bovine serum albumin; 2-Abu, 2-aminobutyric acid; β -Aa, beta-aminoalanine.

FIGURE LEGENDS

Fig 1. Multiple sequence alignment of YbaK superfamily. Multiple sequence alignment of members of the YbaK superfamily performed using the ClustalW Multiple Sequence Alignment Realign program {Thompson, 1994 #289}. The alignment of YbaK, INS domain of prokaryotic-like ProRS, and PrdX is shown. Functionally important residues in *E. coli* ProRS for editing are indicated by a dagger (†) {Wong, 2002 #225}. The residues in *H. influenzae* YbaK investigated by mutagenesis in this study are indicated by an asterisk (*). Residues are colored as follows: red, strictly conserved in YbaK, INS and PrdX; pink, highly conserved in YbaK/INS; green, highly conserved in INS; blue, highly conserved in YbaK; yellow, partially conserved in YbaK; gray, not conserved but selected for mutagenesis. The abbreviations used are: Ec, *Escherichia coli*; Hi, *Haemophilus influenzae*; Ef, *Enterococcus faecalis* V583; Cc, *Caulobacter crescentus* CB15; At, *Agrobacterium tumefaciens*; INS, editing domain of bacterial ProRS.

Fig 2. Computational model of *H. influenzae* YbaK-CCA-Cys complex. **A.** The electrostatic potential surface of YbaK was generated by APBS software {Baker, 2001 #363}. The cysteine moiety of the substrate (yellow) is located in a deep cleft in the active site. **B.** Ribbon representation of YbaK structure with CCA-Cys substrate shown primarily in black. The NNQHF loop, GXXXP loop, and the KRG loop are highlighted in yellow, red, and cyan, respectively. Residues changed in this study are highlighted in purple (deacylation rate decreased >5-fold upon mutagenesis) or green (deacylation rate affected <3-fold upon mutagenesis).

Fig. 3. Views of Docked YbaK-CCA-Cys complex showing predicted H-bonds (dashed lines) between YbaK and the substrate. **A.** H-bonds between Lys46 and A76 phosphate; **B.** H-bonding interactions of C75 phosphate; **C.** H-bonding interactions of A76 adenine; **D.** H-bonds between amino group of substrate cysteine and Tyr20 and Ser129 hydroxyl groups. Colors for atoms used are: black, carbons of CCA-Cys substrate; cyan, phosphorous; red, oxygen; white, hydrogen; gray, carbons of YbaK residues; yellow, sulfur.

Fig. 4. Substrate specificity of *H. influenzae* YbaK. **A.** Structures of amino acids tested as substrates for post-transfer editing by *H. influenzae* YbaK. 2-Abu is 2-aminobutyric acid, β -Aa is β -aminoalanine and Sec is selenocysteine; ++, hydrolyzed; +, hydrolyzed (deacylation activity is ~10 fold reduced relative to Cys-tRNA); -, not hydrolyzed (deacylation activity >100-fold reduced relative to Cys-tRNA). **B.** Deacylation of 2-Abu-tRNA^{Pro} by *H. influenzae* YbaK (0.5 μ M). Hydrolysis in the absence of protein or in the presence of 2 M NaOH is also shown. **C.** Mischarging of β -Aa onto 10 μ M tRNA^{Pro} by 1.5 μ M *E. coli* K279A ProRS in the absence or presence of WT *H. influenzae* YbaK (2 μ M). **D.** YbaK (0.1 μ M) deacylation of 0.5 μ M Cys-tRNA^{Pro} in the absence (YbaK only) and presence of increasing concentrations of Ser-tRNA^{Pro}. **E.** Deacylation of 2'-dA76 or 3'-dA76 Cys-tRNA^{Cys} by WT *H. influenzae* YbaK (1 μ M). Hydrolysis of WT Cys-tRNA^{Cys} by YbaK or 2 M NaOH is also shown. *Inset.* Deacylation of [³⁵S]Cys-tRNA^{Cys} by *E. coli* YbaK (0.5 μ M) in the absence (YbaK only) and presence of Cys-tRNA^{Cys} (WT) and Cys-2'dA76-tRNA^{Cys} (2'dA76) at 30 °C. Axis labels are the same as in the main figure.

Fig. 5. Analysis of deacylation reaction by TLC and LC/MS. **A.** Reaction products of [³⁵S]-Cys-tRNA^{Pro} deacylation by *H. influenzae* YbaK detected by cellulose TLC. Eluent and carrier solvents were n-butanol:acetic acid:water (4:1:1, v/v/v) and methanol, respectively. A unique product band ($R_f = 0.21$, lane 3-5, product) distinct from free cysteine ($R_f = 0.15$, lane 6) is observed. Lane 1: deacylation reaction in the absence of YbaK; lane 2-5: deacylation reaction in the presence of YbaK at 0, 10, 20 and 30 min; lane 6: authentic [³⁵S]-cysteine; lane 7; [³⁵S]-cystine. **B.** LC traces of crude reaction mixtures following *H. influenzae* YbaK-catalyzed Cys-tRNA^{Pro} deacylation (black) or a control reaction in the absence of YbaK (gray). Free cysteine eluted at 1 min and cysteine methyl ester eluted at 3.5 min.

Fig. 6. Possible Cys-tRNA^{Pro} hydrolysis mechanisms. **A.** Water hydrolysis pathway. The free product cysteine formed does not react with methanol (carrier solvent in ESI-MS). **B.** Hydrolysis by cyclization of cysteine. The cysteine thiolactone intermediate reacts with methanol to form cysteine methyl ester.

Fig. 7. Deacylation of aminoacyl-tRNAs by *E. coli* YbaK. **A.** Deacylation of ~1 μ M Cys-3'-[³²P]-tRNA^{Cys} and Sec-3'-[³²P]-tRNA^{Cys} by 5 μ M WT *E. coli* YbaK at 25 °C. A representative buffer (0.15 M KPO₄, pH 7.0) hydrolysis is also shown. **B.** Deacylation of [³⁵S]Cys-tRNA^{Cys} by *E. coli* YbaK (0.5 μ M) in the absence (YbaK only) and presence of Cys-tRNA^{Cys} and Sec-tRNA^{Cys} at 25 °C.

Fig. 8. Summary of interactions in the substrate binding pocket of *H. influenzae* YbaK based on computational and experimental results. A polar environment formed by residues Thr66, Ser44, and Ser136 may lower the pK_a of the cysteine thiol. The thiolate thus generated attacks the carbonyl center, leading to the cleavage of the ester bond and formation of a 4-membered cyclic thiolactone intermediate. The tetrahedral oxyanionic transition state is stabilized by Thr47, Ser129, and the 2'-OH of A76 of the tRNA. Tyr20 is involved in a hydrogen bonding network with the substrate amine group and the hydroxyl group of Ser136. The universally conserved Lys46 residue stabilizes the proper substrate orientation via interaction with the backbone A76 phosphate. The most critical residues or functional groups are labeled in red font. Alanine substitution resulted in deacylation efficiency decreases of ≥ 66 -fold (red font), 21- to 45-fold (blue font), 4- to 6-fold (green font), and ≤ 2 -fold (gray font).

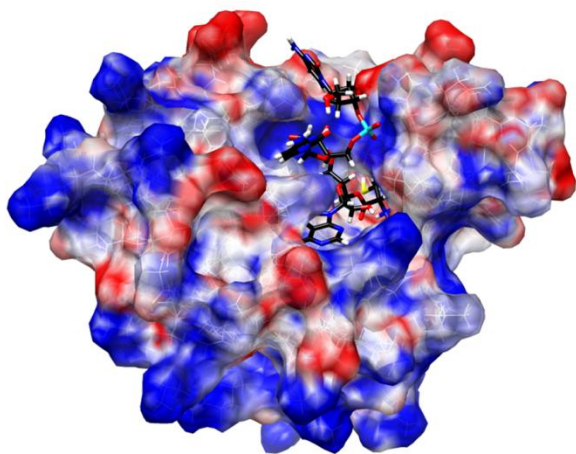
Table 1. Observed rate constants (k_{obs}) for Cys-tRNA^{Pro} deacylation by WT and mutant *H. influenzae* YbaK.

Mutant	$k_{\text{obs}} \times 10^2$ (min ⁻¹) ^a	Fold decrease
WT	31.6 ± 0.74	-
Y20A	0.70 ± 0.02	45
F29A	1.09 ± 0.03	29
S44A	24.74 ± 2.66	1.3
K46A	0.48 ± 0.08	66
K46R	0.71 ± 0.16	44
K46I	0.83 ± 0.07	38
T47A	1.53 ± 0.03	21
T66V	15.30 ± 1.23	2.1
G101A	0.89 ± 0.08	36
S129A	5.68 ± 0.13	5.6
G131A	1.14 ± 0.03	28
G134A	4.29 ± 0.08	7.4
S136A	8.67 ± 0.12	3.6
S136H	1.93 ± 0.03	16

^aThe k_{obs} (min⁻¹) values were calculated by fitting the percent Cys-tRNA^{Pro} remaining as a function of time to a first-order exponential decay equation, $y = Ae^{-k_{\text{obs}} \times t} + B$. Values represent the average of three trials with the standard deviation indicated.

Figure 2

A



B

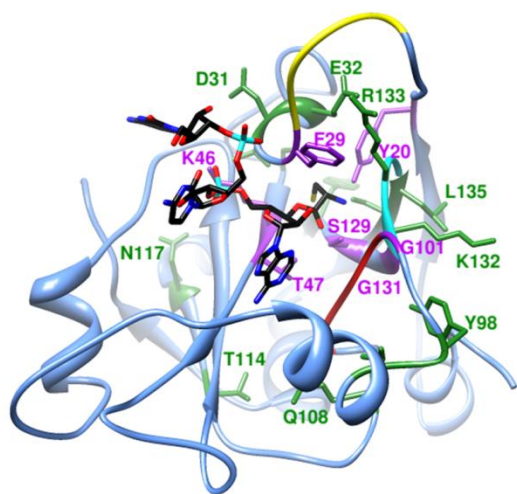
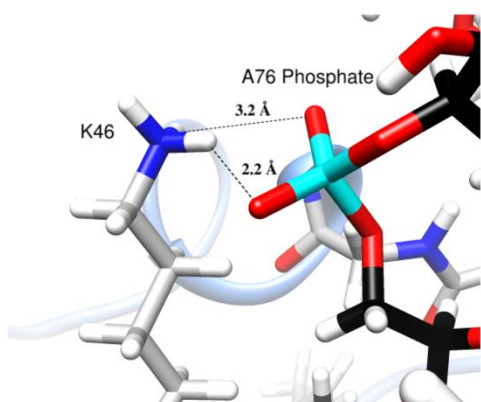
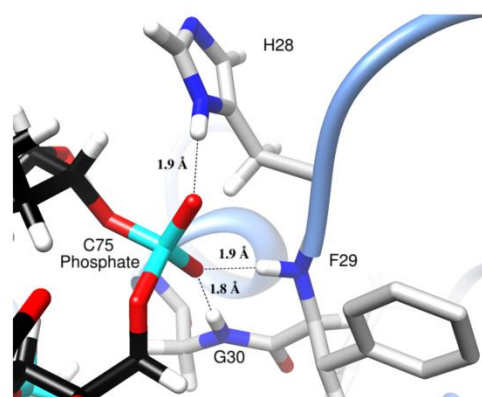


Figure 3

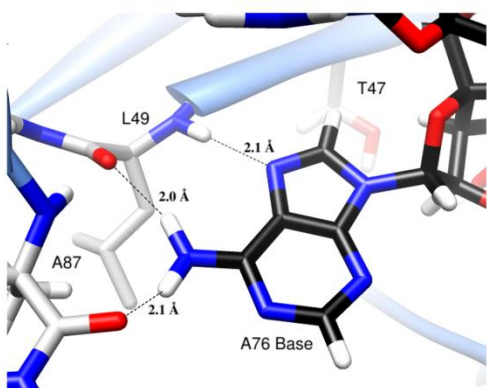
A



B



C



D

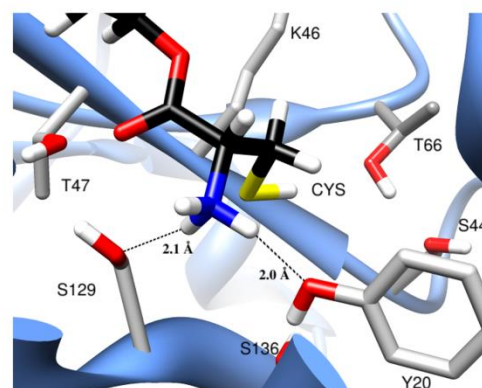


Figure 4

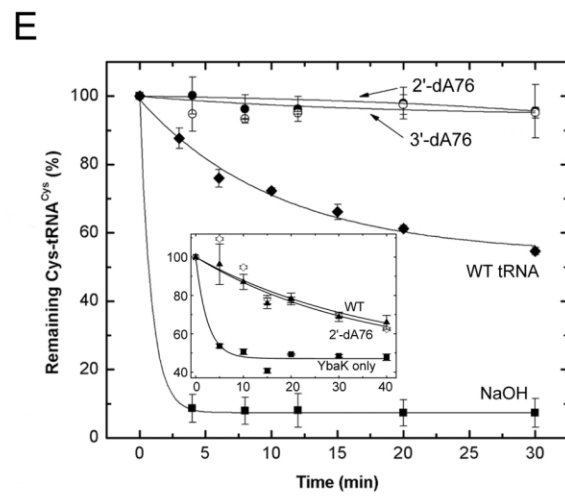
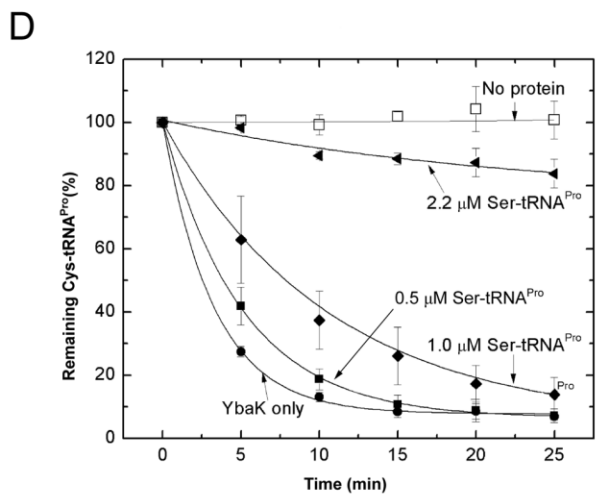
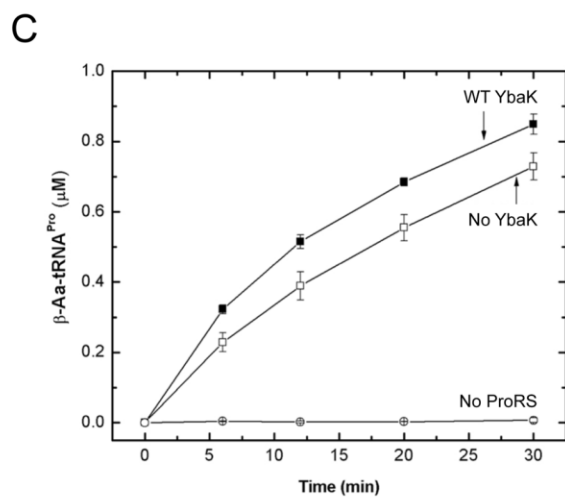
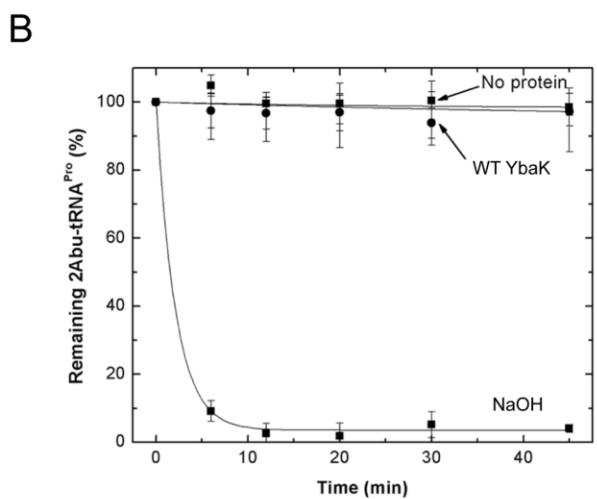
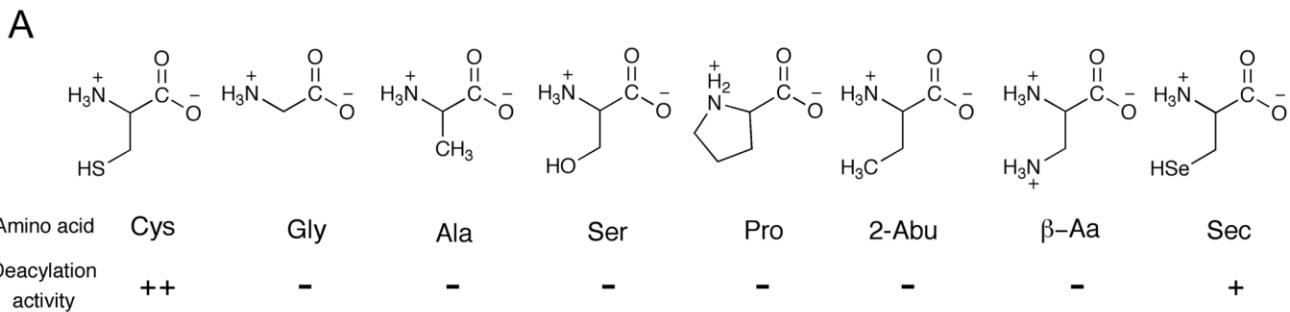
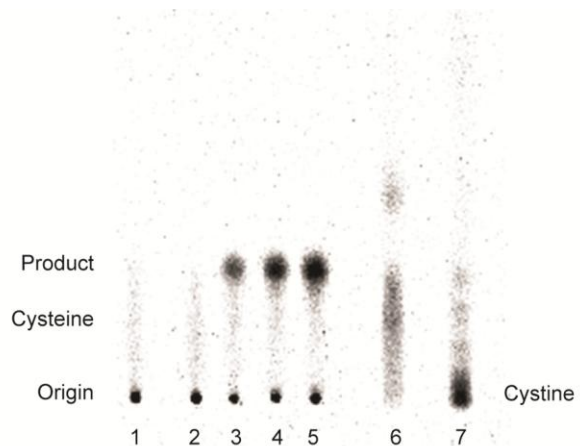


Figure 5

A



B

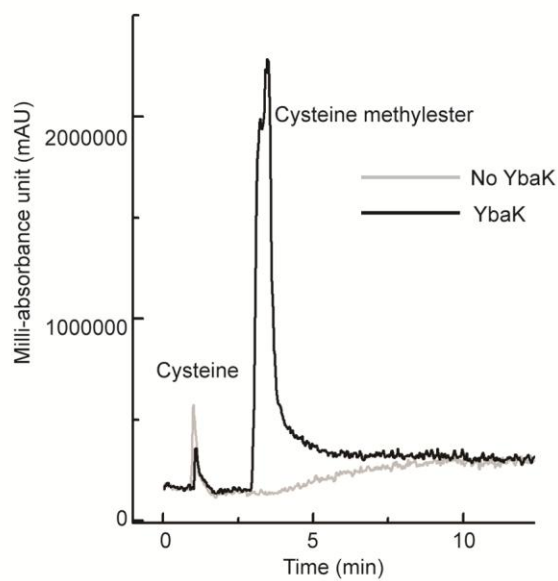


Figure 6

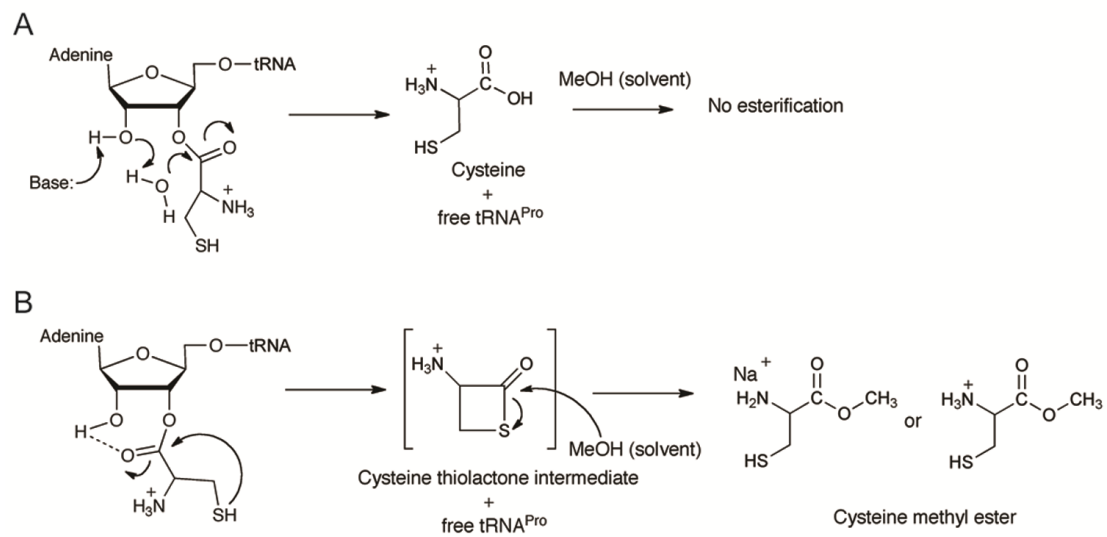


Figure 7

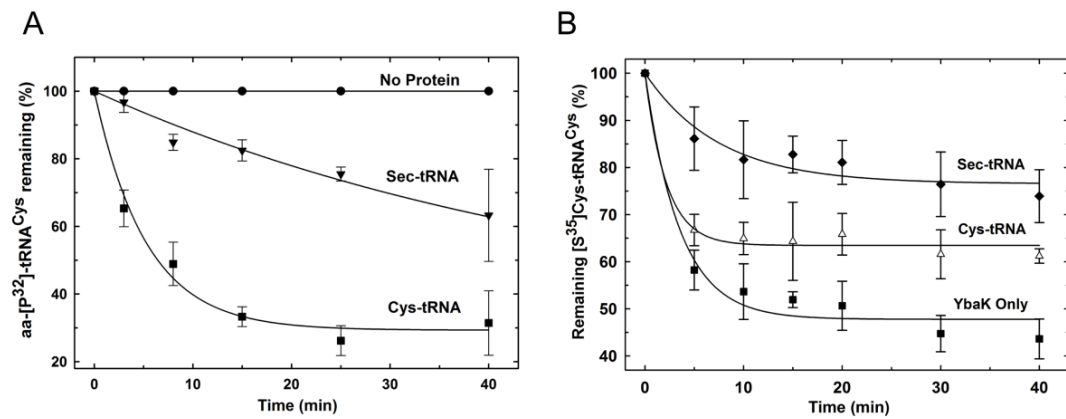


Figure 8

